

COMPUTATIONAL FLUID DYNAMIC MODELLING OF CAVITATION

Manish Deshpande,[†] Jinzhang Feng,[‡] Charles L. Merkle*
 Propulsion Engineering Research Center
 Department of Mechanical Engineering
 The Pennsylvania State University

SUMMARY

Models in sheet cavitation in cryogenic fluids are developed for use in Euler and Navier-Stokes codes. The models are based upon earlier potential-flow models but enable the cavity inception point, length and shape to be determined as part of the computation. In the present paper, numerical solutions are compared with experimental measurements for both pressure distribution and cavity length. Comparisons between models are also presented. The CFD model provides a relatively simple modification to an existing code to enable cavitation performance predictions to be included. The analysis also has the added ability of incorporating thermodynamic effects of cryogenic fluids, into the analysis. Extensions of the current two-dimensional steady state analysis to three-dimensions and/or time-dependent flows are, in principle, straightforward although geometrical issues become more complicated. Linearized models, however offer promise of providing effective cavitation modeling in three-dimensions. This analysis presents good potential for improved understanding of many phenomena associated with cavity flows.

COMPUTATIONAL MODEL

Cavitation is a persistent problem in many fluid mechanical devices and has received much attention in the past several decades [1, 2]. In many cases cavitation occurs in flows that include rotational effects, viscous effects and heat transfer. Existing models based on potential flow theory are relatively limited in the ability to analyze these more complex flowfields. The objective of the present research is to extend the potential flow analyses to solutions of the Euler/Navier-Stokes equations to predict the geometrical characteristics of the cavity. It requires no presumptions of either the cavity length or cavity inception point and satisfies the cavity pressure as well as normal velocity condition on the cavity surface.

The steady state Navier-Stokes equations when written in a strongly conservative form in generalized coordinates using the unsteady artificial compressibility formulation become

$$\Gamma \frac{\partial Q}{\partial \tau} + \frac{\partial}{\partial \xi}(E - E_v) + \frac{\partial}{\partial \eta}(F - F_v) = 0 \quad (1)$$

where Q is the vector of primary dependent variables, E and F are the convective fluxes in the ξ and η directions respectively and E_v and F_v are the viscous fluxes. The Euler equations are obtained from the above by dropping the viscous flux terms. Turbulence effects are calculated from the Baldwin-Lomax algebraic turbulence model [3].

[†] Graduate Research Assistant

[‡] Research Associate

* Distinguished Alumni Professor

An explicit time-marching Runge-Kutta algorithm is used to advance the Navier-Stokes/coupled energy system of equations in pseudo-time. Center-differencing is used for all spatial derivatives. Local time-stepping is used to improve convergence. A fourth-order artificial viscosity [4] is used to prevent odd-even splitting in the numerical solution.

The inviscid portion of the coupled equations becomes hyperbolic with the addition of the artificial time derivative. This enables the use of the Method of Characteristics (MOC) procedure to formulate the inflow and outflow boundary conditions, analogous to compressible flow. The application of MOC to the above problem dictates that the inflow be determined by three boundary conditions and one characteristic equation and the outflow by one boundary condition and three characteristics. Here the total pressure, the inflow angle and the temperature are specified at the inlet, while the static pressure is specified at the downstream boundary. These are complemented by information obtained from outrunning characteristics.

Boundary conditions at the body surface in the absence of cavitation are the no-slip condition for the NS equations and inviscid wall conditions for the Euler equations, and a specified wall temperature or heat flux condition. These are augmented by applying the normal momentum equation on the surface. Boundary conditions on the cavity interface are discussed in the next section.

CAVITATION MODEL

The cavity is modeled as a region of constant pressure, corresponding to the liquid vapor pressure. The location of the cavity interface is determined by over-specifying the boundary relations on it, analogous to procedures used in potential flow models. For the Navier-Stokes equations the boundary conditions include flow tangency, continuity of shear stress at the interface and the cavity pressure. These conditions replace the usual two no-slip conditions ($u = v = 0$), and enable the computation of the interface location as a part of the marching process. In the Euler model the cavitation pressure and the total pressure are specified along with one characteristic.

In keeping with the potential flow models, both a linear and a nonlinear procedure can be used to enforce the cavity conditions. In the linear case the cavity conditions are applied on the airfoil surface, under the assumption of a thin cavity, so that the computational domain does not change. For the nonlinear procedure, the cavity conditions are applied directly on the cavity interface. As a consequence the computational domain adjacent to the cavity evolves and needs to be updated.

During the computational procedure the pressure distribution is checked against the specified cavitation pressure. If the pressure at any point drops below the local vapor pressure that point is switched from a 'solid wall' point to a 'cavity' point with a corresponding switch in the boundary conditions. Subsequent iterations then allow the normal velocity on the cavitating interface to deviate from zero. The finite normal velocity on the interface can then be used to update the cavity interface.

The cavity profile is fixed by ensuring positive cavity thickness at every cavitating point. Any points with negative cavity thickness are reset to non-cavitating points in the next iteration regardless of their pressure level. This enables the cavity to shrink if required by the iterative procedure. If the cavity ends with a finite non-negative thickness the cavity is artificially closed by adding an afterbody [5, 6], which is treated as inviscid. The afterbody shape chosen here is a cubic profile that merges tangentially with the body surface.

In the nonlinear analysis the grid is then updated to incorporate the change in the airfoil/cavity boundary. In the next iteration the computations are performed over the modified grid. The non-cavitating points are treated as standard, while the interface points are treated as constant pressure points. This procedure is then repeated. The cavity surface then converges to a unique solution satisfying both flow tangency and pressure conditions. In the linear analysis, the solution is obtained in exactly the same manner as above, without updating the grid.

THERMODYNAMIC ANALYSIS

The thermal effects of cavitation result from the continuous vaporization process that is needed to sustain the cavity on the body surface. The heat for this vaporization must be extracted from the bulk liquid, and as a result, the temperature of the liquid in the immediate vicinity of the liquid-vapor interface is depressed below the free-stream temperature. An energy balance at the cavity interface yields the numerical conditions required for incorporating the thermal effects into the cavitation model. The evaporation rate and the temperature depression is determined by the thermal boundary layer at the liquid-vapor interface. The local temperature depression reduces the local vapor pressure of the fluid, which leads to a lower observed cavity pressure. As a result, the cavity size is smaller with temperature depression effects present.

Thermodynamic effects of cavitation are generally more significant in cryogenic fluids than in room temperature fluids such as water, because they are typically operated closer to their critical point. In addition, the slope of the vapor pressure-temperature curve of cryogenic fluids is much steeper than that for water. As a result, the change in vapor pressure is more significant.

RESULTS AND DISCUSSION

The cavitation model and the computational procedures presented above are discussed in greater detail elsewhere [7, 8, 9]. Comparisons of the Euler and Navier-Stokes models with experiments and potential flow calculations and with each other as well as parametric studies of cavitation are also presented in the above references. Some representative results are shown here.

Figure 1 compares the predicted pressure distribution over a NACA66(MOD) airfoil for the Euler and Navier-Stokes nonlinear analyses with experiment. Although there are some differences, the predictions from both the Navier-Stokes and the Euler analyses agree quite well with experiment and qualitatively with each other.

The cavity length for both the Euler and Navier-Stokes models is plotted as a function of cavity pressure in Fig. 2. The two models predict similar cavity lengths for the shorter cavities but the Euler predictions are slightly larger than the NS predictions at the longer cavity lengths. The obvious implication is that the presence of viscous and turbulent diffusion decreases the cavitation region slightly. One possible explanation is the fact that the fluid over the cavity interface in the viscous case has less energy than the inviscid case, due to viscous effects. The viscous fluid therefore tends to reattach earlier, in comparison to the inviscid fluid. These comparisons though justify the use of either velocity potential or Euler methods in a design model, where cavitation regimes are required to be identified.

A similar comparison between the linear and nonlinear Navier-Stokes cavitation models is shown in Fig. 3, for a NACA0012 airfoil at five degrees angle of attack. The much simpler linear model consistently provides an excellent prediction of the cavity length. The effectiveness of placing the cavity boundary conditions on the body along with the ability to use a fixed grid suggest that the linear analysis is best for design purposes, although periodic checks with the nonlinear model are recommended. The predictions agree quite well for the short cavities. However as the cavity length increases the predictions deviate, as the inaccuracies in the linearization become more significant.

The prediction of midchord cavitation is another advantage of the CFD solution over the velocity potential. For devices where the shape of the pressure distribution resembles a rooftop, the absence of a sharply defined minimum pressure location makes it difficult to identify a cavitation inception point for velocity potential solutions. In the CFD analysis such a pre-specification is not necessary. The prediction of midchord cavitation becomes straightforward, presented in Fig. 4 for a NACA66 hydrofoil at one degree angle of attack, compared with experiments from [10]. The predictions are in good agreement with experiments both with respect to the location of the cavity inception point as well as the length of the cavity. The expected stagnation pressure at the termination of the cavity can also be clearly

seen in the computations. This capability for predicting midchord cavitation represents an important advantage of the model.

As noted before the model needs no presumptions about either the pressure distribution or cavity length. Therefore we next turn to predictions of pressure level (cavitation number) for a computed cavity length. For this, we compare predicted pressure distributions with the data from Hord [11] for liquid hydrogen for a tapered plate airfoil. To compare our predictions we select a cavity length and present in Fig. 5, computed and measured pressure distribution on the airfoil surface. In this case the cavity length is about half the chord. The agreement between the calculation and the experiment is quite satisfactory in terms of the cavitation pressure level.

To evaluate the thermodynamic effects of cavitation, we compare temperature depression predictions with measurements from Hord [11] for liquid hydrogen in Fig. 6. as a function of cavity length. The calculated temperature depressions correspond to three different upstream velocities are shown. The experimental data for hydrogen, which are for a velocity range of about 25 to 55 m/s show non-dimensional temperature depressions up to 0.18. The analysis predicts similar magnitudes (up to 0.16). In addition, the analysis predicts an increase in $\Delta T/T$ with velocity, which is to be expected on theoretical bases, but which cannot be discerned clearly from the experimental data. Similar results were obtained for nitrogen [8].

REFERENCES

- [1] Tulin, M. "Steady two-dimensional cavity flows about slender bodies," Tech. Rep. 834, David Taylor Model Basin, 1953.
- [2] Wu, T. "Cavity and Wake Flows," *Annual Review of Fluid Mechanics*, vol. 4, 1972.
- [3] Baldwin, B., and Lomax, H. "Approximate and Algebraic Model for Separated Turbulent Flows," AIAA Paper 78-257, AIAA, 16th Aerospace Sciences Meeting Huntsville, AL. January 1978.
- [4] Kwak, D., Chang, J., Shanks, S., and Chakravarthy, S. "A Three-Dimensional Navier-Stokes Flow Solver Using Primitive Variables," *AIAA Journal*, vol. 24, 1986, 390–396.
- [5] Tulin, M., and Hsu, C. "New Applications of Cavity Flow Theory," Proc. 13th Symposium on Naval Hydrodynamics, Tokyo 1980.
- [6] Buist, J., and Raven, H. "A Consistently Linearized Approach for the calculation of Partial Sheet Cavitation," *Cavitation and Multiphase Flow Forum, ASME, FED*, vol. 98, 1990.
- [7] Deshpande, M., Feng, J., and Merkle, C. "Cavity Flow Predictions Based on the Euler Equations," *Journal of Fluids Engineering*, to appear, 1993.
- [8] Deshpande, M., Feng, J., and Merkle, C. "Numerical Modeling of the Thermodynamic Effects of Cavitation," 3rd International Conference on Cavitation, Cambridge, U.K. December 1992.
- [9] Deshpande, M., Feng, J., and Merkle, C. "Navier-Stokes Analysis of 2-D Cavity Flows," *Cavitation and Multiphase Flow Forum*, Washington, D.C. June 1993.
- [10] Shen, Y., and Dimotakis, P. "The influence of surface cavitation on hydrodynamic forces," Proc. 22nd ATTC, St. Johns 1989.
- [11] Hord, J. "Cavitation in Liquid Cryogenics: 2-Hydrofoils," Tech. Rep. CR-2156, NASA, 1972.

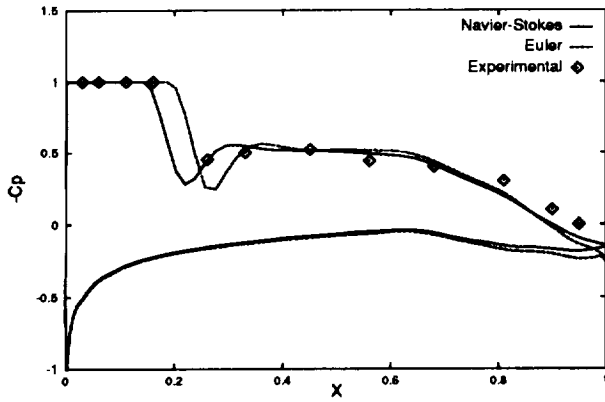


Figure 1: Comparison between Euler and Navier-Stokes analyses for NACA66(MOD) airfoil at $\alpha = 4$ deg. and $\sigma = 1.0$

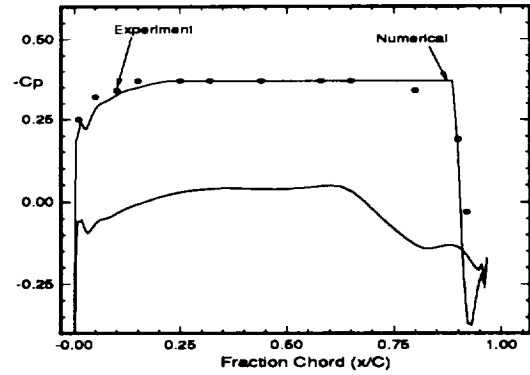


Figure 4: Mid Chord Cavitation for NACA66(MOD) airfoil at $\alpha = 1.0$ and $\sigma = 1.0$.

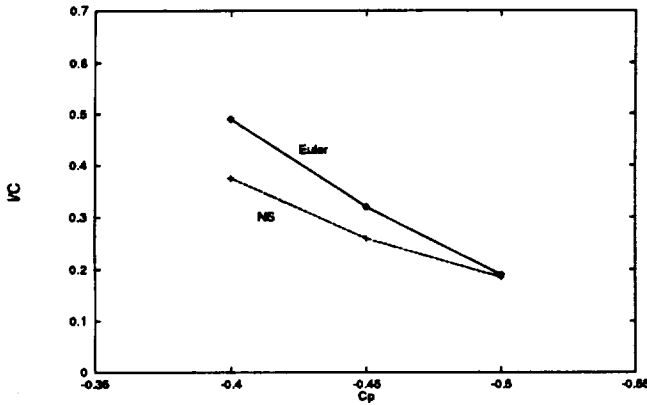


Figure 2: I/C vs C_p for Navier-Stokes and Euler models for a NACA66(MOD) airfoil at four degrees angle of attack

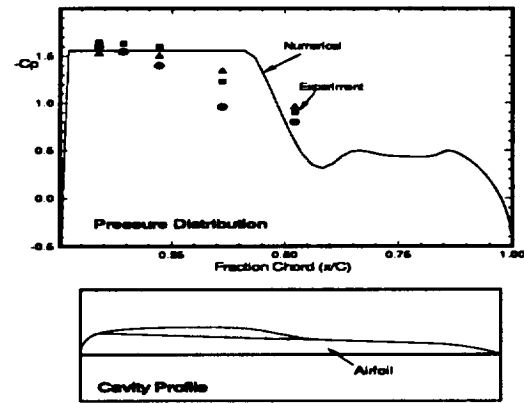


Figure 5: Comparison of cavitation pressure level with measurements from Hord.

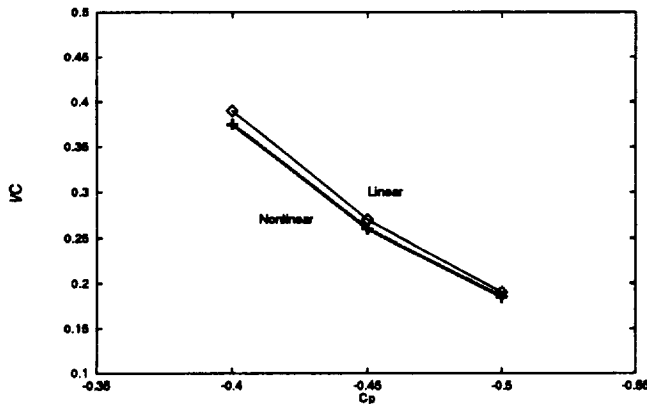


Figure 3: I/C vs C_p for linear and Nonlinear Navier-Stokes Models for NACA0012 Airfoil

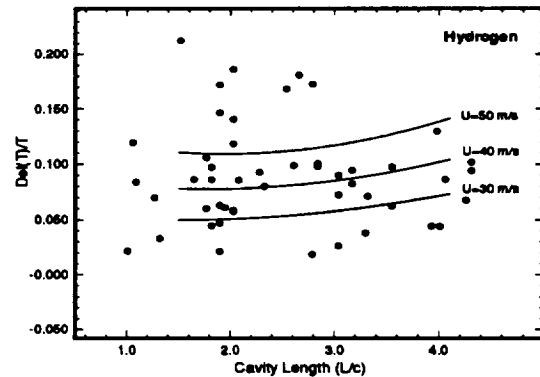


Figure 6: Temperature Depression as a function of Cavity Length for Hydrogen Comparison with Hord